ISSN 1330-3651 (Print), ISSN 1848-6339 (Online)
https://doi.org/10.17559/TV-20230424000563
Original scientific paper

Generation of Non-Iterative POHs based on Optimized Hybrid Phase for Fresnel Lensless Holographic Projection

Min FAN, Jiaxuan WANG, Chengtao DU, Jin YANG*, Haibo WANG, Xiaoli XU

Abstract: Phase-Only Holograms (POHs) are widely embraced for their advantages, including high quality reconstruction and high diffraction efficiency. However, when generating POHs, the utilization of solely random or quadratic phase often leads to speckle noise and ringing artifacts in reconstructed image. To tackle this issue, this paper introduces a non-iterative Optimized Hybrid Phase-only Holograms (OHPOHs) algorithm designed for Fresnel Lensless Holographic Projection system. The proposed algorithm consists of three steps. Firstly, selected quadratic phase and random phase are combined with an appropriate weight coefficient to create a hybrid phase. Next, the hybrid phase is iteratively optimized. Lastly, a complex amplitude is formed by combining the optimized hybrid phase and arbitrary target image, resulting in the generation of POHs through a single-step calculation. Additionally, this paper explores the process of selecting an appropriate weight coefficient for the phase blending procedure. Numerical experiments demonstrate that the non-iterative OHPOHs achieves superior reconstruction of high-quality images by effectively suppressing speckle noise and ringing artifacts. Moreover, this improvement is achieved while maintaining computation efficiency comparable to that of the Optimized Random Phase (ORAP) algorithm and the Hybrid Phase-Only Hologram (HPOHs) algorithm.

Keywords: fresnel lensless holographic projection; non-iterative algorithm; optimized hybrid phase mask; phase only holograms

1 INTRODUCTION

Holographic display, a highly promising display technology, has captured significant attention from researchers [1-4]. One advancement in this field is Computer Generated Holograms (CGHs) [5-7], which distinguish themselves from traditional optical holograms by not relying on physical objects. Instead, they enable the reproduction of virtual objects through digital quantitative calculation. CGHs offer numerous advantages, including precision, flexibility, ease of replication, and find a wide range of applications [8, 9].

Within the realm of CGHs, Phase-only Holograms (POHs) surpass Amplitude-only Holograms (AOHs) in terms of diffraction efficiency and contrast enhancement. As a result, the prevalent method for implementing computer-generated holograms involves combing coherent light sources with phase-only Spatial Light Modulators (SLMs) or Liquid Crystal on Silicon (LCOS) [10, 11]. These SLMs or LCOS are loaded with POHs, and when illuminated with coherent light, they generate the reconstructions on the image plane. Therefore, the crucial role of POHs directly influences the quality and the generation speed of the reconstruction. The investigation of generation algorithms for POHs is a research direction that has garnered considerable attention among researchers.

POHs are generated using algorithms, which can be classified into two main categories: iterative algorithms and non-iterative algorithms. Among these, the Gerchberg-Saxton (GS) [12] is a well-known iterative algorithm for obtaining the phase of an image. This algorithm iteratively refines the complex amplitude between the diffraction plane and the observation plane to derive the phase of the target image. Over the years, scholars have made notable advancements in the GS algorithm, aiming to enhance convergence speed and improve the quality of the reconstruction. One notable improvement is the Fienup algorithm [13], which enhances the reconstructed image quality by augmenting the amplitude constraint. However, it relies on manually adjusting the feedback coefficient, which is a drawback. To address this limitation, the GS algorithm with Weight Coefficients (WGS) [14] introduces adaptive changes to the coefficient, thereby constraining the amplitude distribution of the signal region during the iterative. Nevertheless, the WGS algorithms suffer from unstable feedback. To ensure convergence and stability, the Adaptive Weighted GS (AWGS) algorithm [15] incorporates an exponential term in the feedback mechanism. In GS-based algorithms, the initial random phase can introduce speckle noise.

To improve the reconstruction quality, many algorithms, such as Double Constraints algorithm [16], Error Diffusion Algorithm [17], hybrid iterative algorithm [18] are proposed. Although these algorithms yield higher-quality reconstructed images, their iterative nature results in longer processing time and low convergence speed due to repeated iterations. Consequently, their application is limited in real-time 3D display and situations where there are real-time changes in incident light fields. To address this challenge, researchers are actively exploring alternative algorithms that can achieve faster processing and real time processing capabilities for POH.

In comparison to iterative algorithms, non-iterative algorithms offer advantage of requiring only a single calculation step, making them well-suited for real-time display requirements. Random Phase (RAP) mask algorithm [19], one of the typical non-iterative mask-based algorithms, generates a relatively high-quality reconstructed holograms, which is on the ground that the POHs in RAP act as high pass filters, reconstructing the low-frequency components and outline of the target image while sacrificing finer details. RAP mask algorithm is employed to disperse wavefront information across the hologram, enhancing reconstruction quality [20]. However, the presence of singular points in the random phase produces noticeable speckle noise in reconstructed image.

A non-iterative algorithm proposed by Alejandro in 2018, combines the iterative algorithm-GS algorithm with the non-iterative algorithm-Optimized Random Phase

(ORAP) [21, 22] mask algorithm, which uses the GS algorithm to calculate the ORAP mask for an optical system with known parameters and then form a complex amplitude for any target image. the optimized phase was used in Alejandro's algorithm to generate POHs non-iteratively. However, the reconstructed holograms generated by the algorithm still produce a relatively amount of speckle noise owing to the initial random phase.

Another algorithm involves employing the quadratic phase mask. For example, in 2020, Chen employed iterative algorithm based on quadratic phase mask as the initial phase in a Fourier holographic system to obtain optical phase mask and eventually generate POHs by one-step calculation [23]. While Chen's algorithm effectively suppresses speckle nose, it may introduce ringing artifacts parallel to the contour edges in the reconstructed holograms.

To address the challenge of ringing artifacts, Shen proposed the Hybrid-Phase-Only Holograms (HPOHs) algorithm in 2022 [24], which combines random phase with quadratic phase to form a hybrid phase, leveraging the advantages of both types of phases to improve reconstruction quality and diffraction efficiency. However, this algorithm is still applicable to Fourier holographic systems, and there is still room for improvement in the reconstruction quality.

Additionally, some scholars enhance reconstruction quality by zero-padding the target image, creating rectangular holes around it. The Mixed-Region Amplitude Freedom (MRAF) algorithm [25, 26] regards the target image as the signal region and the zero-padded region as the non-signal region, employing different constraint strategies in each region to improve reconstruction accuracy.

In 2017, Mehrabkhani introduced an improved GS algorithm, specifically designed for the Fresnel holographic system [27]. This algorithm significantly improves the quality of reconstructed images and faster convergence by using dynamic zero-padding in the input and output images. However, an amount of time is consumed in this algorithm.

Apart from mask-based algorithms, there are non-iterative algorithms available for suppressing speckle noise. One such algorithm is the Time-Division Multiplexing (TDM) [28], which employs high-speed switching and display of different holograms by using SLMs to reconstruct holograms. Another algorithm, which can generate reconstructed images in relatively high quality, is the Complementary Phase-Only Holograms algorithm [29, 30]. However, these algorithms come with challenges such as high computational complexity and the requirement for high-performance SLMs.

To address the need for generating high-quality POHs directly, researchers have proposed alternative algorithms such as the Direct Search algorithm [31], Simulated Annealing Algorithm [32], and Genetic algorithm [33]. These algorithms aim to search for pixel values that minimize the error between the reconstruction and the target. They can yield results that closely approximate the global optimal solution and are compatible with other algorithms. However, these algorithms demand significant computational resources and substantial storage space.

The algorithms motioned above, such as ORAP, MRAG, and HPOHs, are all based on the Fourier Holographic Projection system. This system is a quasi-4f system, which can effectively eliminate the DC noise caused by the pixelated structure of SLMs in reconstructed image. however, the optical path system in these algorithms is relatively complex [34-36]. Fresnel holography system means that coherent plane light illuminates the holographic plane, and the light waves propagate freely for a certain distance to reach the image plane, where the reconstruction is generated. There is no lens between the hologram plane and the image plane, which makes Fresnel Holography system have a simple optical path and don't require high-performance SLMs, making it widely applicable [37-39].Therefore, researching POHs generation algorithms that are suiable for Fresnel Holographic Lensless Projection systm, do not require high-performance SLMs, and possess a balance between computation efficiency and achieving superior hologram quality is a promosing task.

Based on the above work, this paper proposes an Optimized Hybrid Phase-Only Holograms (OHPOHs) algorithm, which is suitable for generating high-quality POHs in a Fresnel diffraction projection holographic system. For a given optical system, the appropriate quadratic phase and random phase are mixed according to weight parameters before generating POHs. The hybrid phase is then iteratively optimized to make the distribution of the phase smoother. Multiply the optimized hybrid phase with the target phase to obtain complex amplitude, and then only one step is needed to obtain POHs. Numerical experiments show that this algorithm has two advantages. First, it improves the of the reconstructed quality by suppressing both the speckle noise and the ringing artifacts. Second, it has a fast hologram generating speed as it can compute the optimized hybrid phase prior to generating images, allowing for quick genration of POHs based on diferent target images.

2 BACKGROUND KNOWLEDGE

As the POHs generated by the OHPOHs proposed in this paper are suitable for Fresnel lensless holographic projection system, an introduction to the mechanism of this system is needed. The problems and chanllenges associated with non-iterative algorithms will also be analyzed in this part.

2.1 Mechanism of Fresnel Lensless Holographic Projection System

The mechanism of Fresnel lensless holographic projection system is shown in Fig. 1. Coherent plane light illuminates the holographic plane, and the light waves propagate freely for a certain distance to reach the image plane, where the reconstruction is generated. There is no lens between the two planes. The hologram generates the reconstructed image through Fresnel diffraction (FD), and the algorithm used for the FD integral is Single Fast Fourier Transform (S-FFT) [40], its equation is shown in Eq. (1):

$$g(x,y)=\frac{\exp(x,y)}{jg\lambda}\exp\frac{jk}{2d}\left(x^2+y^2\right)\cdot \cdot FFT\left[G(u,v)\exp\frac{jk}{2d}\left(u^2+v^2\right)\right] \tag{1}$$

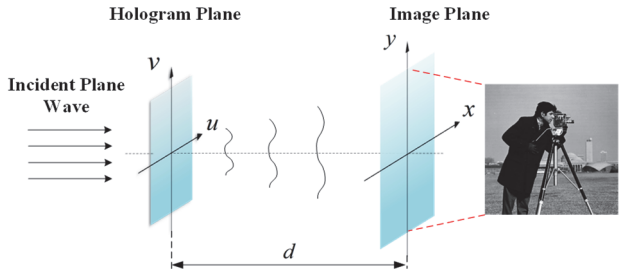

Figure 1 Mechanism of lensless holographic projection with Fresnel diffraction

In Eq. (1), $g(x, y)$ represents the complex amplitude of the image plane, x and y are the horizontal and vertical coordinates of the image plane respectively. $G(u, v)$ represents the complex amplitude hologram on the hologram plane, u and v are the coordinates of the hologram plane. λ is the wavelength of the incident coherent plane wave, $k = 2\pi/\lambda$ is the wavenumber, d is the diffraction distance, and FFT [.] denotes the Fast Fourier Transform (FFT). In this paper, the process of free propagation of the wave from the hologram plane to the image plane is referred to as FD.

It should be noted that the size of the image plane is not the same as the size of the hologram plane. The size of the image plane is related to the size of the hologram plane and the d, as shown in Fig. 2.

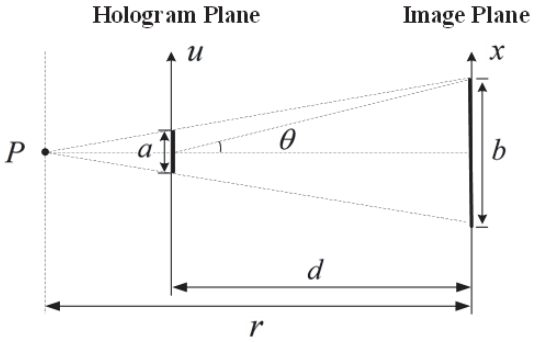

Figure 2 Geometric relationship between holographic plane and image plane

If the resolution of the hologram is $M \times N$, with a sampling interval that is the same as the pixel size of SLMs, which is ΔSLM. For the convenience of the analysis, the following analysis is based on the one-dimensional analysis. The hologram has a side length of $a = M \times \Delta SLM$. The highest spatial frequency of the hologram is:

$$u_{\max}=\frac{M}{2a}=\frac{M}{2M\cdot\Delta SLM}=\frac{1}{2\cdot\Delta SLM} \tag{2}$$

The resolution of the image plane is consistent with that of the hologram, which is $M \times N$. Different points (x, y) on the image plane correspond to light with different spatial frequencies on the hologram plane, that is, light in different directions. Therefore, $u_{\max}$ is related to the side length b in the x direction of the image plane:

$$u_{\max}=\frac{\sin\pi/2-\theta}{\lambda}\approx\frac{1}{\lambda}\cdot\frac{b/2}{d} \tag{3}$$

Combining Eq. (2) and Eq. (3), we can obtain:

$$b=\frac{\lambda d}{\Delta SLM} \tag{4}$$

Obviously, the sampling interval of the image plane is:

$$\Delta x=\frac{b}{M}=\frac{\lambda d}{M\cdot\Delta SLM} \tag{5}$$

Now we will analyze the case where the coherent light wave propagates from the image plane to the hologram plane, which is referred to as Inverse Fresnel diffraction (IFD) in this paper. The hologram's complex amplitude $G(u, v)$ can be calculated using Eq. (6):

$$G(u,v)=\frac{\exp(-jk\lambda)}{-jd\lambda}\exp\left[-\frac{jk}{2d}\left(u^2+v^2\right)\right]\cdot \cdot IFFT\left[g^*(x,y)\exp\left[-\frac{jk}{2d}\left(x^2+y^2\right)\right]\right] \tag{6}$$

Here, $IFFT[\cdot]$ is the Inverse Fast Fourier Transform ($IFFT$) and $g(x, y)^*$ is the conjugate of $g(x, y)$. The highest spatial frequency $x_{\max}$ of the image plane is:

$$x_{\max}=\frac{1}{2\Delta x}=\frac{M\cdot\Delta SLM}{2\lambda d} \tag{7}$$

It should be noted that S-FFT is suitable for the case of long diffraction distance d, which needs to satisfy Eq (8), otherwise under-sampling will occur.

$$d\geq\frac{N\cdot(\Delta SLM)^2}{\lambda} \tag{8}$$

2.2 Challenges in Non-Iterative POHs Algorithms

Although the quality of reconstruction obtained by iterative methods is usually higher, they often require a longer computation time, non-iterative methods have received widespread attention from researchers. These non-iterative algorithms offer various advantages such as computational efficiency, real-time capabilities, and improved quality of reconstructed holograms. However, the challenges lie in exploring algorithms that can efficiently generate high-quality POHs without significantly increasing the computational complexity.

According to previous review in Section 1, even with optimized random phases, the reconstructed images still suffer from significant speckle noise, as shown in Fig. 3b, which is caused by uncontrollable distribution of random phase in certain non-iterative algorithms. While employing quadratic phase as the phase mask in mask-based algorithms can make the phase distribution smoother and suppress the speckle noise. Although the speckle noise is

suppressed, there are obvious ringing artifacts, as shown in Fig. 3c. Moreover, SLMs-based algorithms demand significant computational resources and large storage space for algorithm procedure, which introduce a low computation efficiency. The above algorithms reviewed in part 1 are mostly based on Fourier holographic projection system, so exploring POHs generation algorithms that is suitable for Fresnel lensless holographic system is a meaningful research direction. Building upon the discussion on challenges in non-iterative algorithm, a hybrid POHs algorithm is necessarily explored to enhance the high quality and computational efficiency.

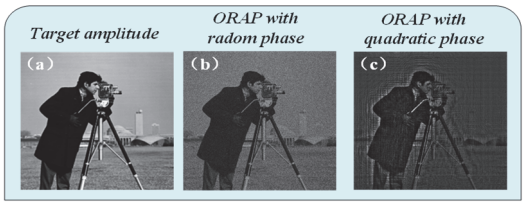

Figure 3 The impact of using random and quadratic phase on the reconstructed image in the ORAP algorithm: (a) Target Image; (b) ORAP with random phase; (c) ORAP with quadratic phase

Therefore, we propose the OHPOHs. First, we analyze the selection of quadratic phase parameters suitable for the Fresnel domain. Then, before generating POHs, the quadratic phase suitable for the given optical system is mixed with random phase in an appropriate proportion to form a phase mask, which is multiplied by a binary function rectangular aperture to form complex amplitude. Then, an improved iterative process is used to optimize the hybrid phase inside the rectangular aperture. Finally, the optimized hybrid phase is used as a phase mask to multiply the amplitude of the target image which is also added with rectangular aperture to form a complex amplitude, and then obtain the POHs by IFD, thus obtaining a high-quality reconstructed image.

3 OPTIMIZED HYBRID PHASE ONLY HOLOGRAM

Before explaining the OHPOHs proposed in this paper, we first introduce how to select the appropriate parameters for the quadratic phase based on the Fresnel holographic system [36, 37]. The reason why the selection of the parameters for the quadratic phase is important is that the bandwidth of the spectrum, which is formed by multiplying the amplitude of the target image with different quadratic phases, varies [20]. Fig. 4. shows mutltipying the same traget image with different quadratic phases results in varying bandwiths of the complex amplitude.Only when the frequency spectrum of the image plane is band-limited, that is when the energy of the entire image is uniformly distributed on the hologram plane, the reconstructed quality can be improved. In other words, the initial quadratic phase should be band-limited, and the bandwidth of the image plane should be equal to the size of the hologram plane. Now, let's specifically discuss the method for setting the quadratic phase parameters.

3.1 Setting of Quadratic Phase Parameters

Quadratic phase mask can be regarded as multiplying the object wave with a virtual convergent wave, as shown in Fig. 2, where r is the distance between the virtual convergent wave focal point P and the image plane, here, this r is the key parameter. In a Fresnel lensless holographic system, the expression for the quadratic phase is as Eq. (8):

$$\varphi_0 = \frac{\pi}{\lambda}\frac{x^2+y^2}{r} \tag{8}$$

according to the geometric relationship between the two plane, the r can be determined:

$$\frac{r-d}{r} = \frac{a/2}{b/2} \tag{9}$$

Here, a is the length of hologram plane, b is the length of image plane, d is the distance between the two planes. That is.

$$r = \frac{d}{1-a/b} \tag{10}$$

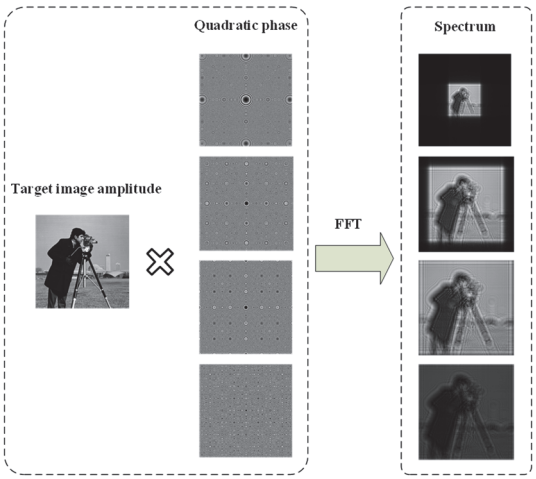

Figure 4 Spectrum of complex amplitude formed by target image amplitude and different quadratic phase

3.2 Flow of OHPOHs Algorithm

In Part 3.1, we have already explained the issue of setting the quadraitc phase parameters. Now, let's elaborate on the OHPOHs algorithm workflow. OHPOHs is mainly divided into three steps, and the algorithm flow chart is shown in Fig. 5.

Step 1: Form the hybrid phase φ_0.

The random and the quadratic phase are mixed according to Eq. (11) to form a hybrid phase:

$$\varphi_0 = (1-C)\cdot\varphi_{rand} + C\varphi_{quad} \tag{11}$$

In this equation, φ_{rand} is the random phase distribution, φ_{quad} is the quadratic phase distribution on the image plane, and C is a weight coefficient, the value is between 0 and 1, which determines the mixing ratio of these two phases. The value of C is important because if it is close to 1, there will be more quadratic phase components in the reconstruction, and the reconstructed image will be more affected by ringing artifacts. On the other hand, if it is close to 0, the

reconstructed result will be affected by speckle noise. Later, we will discuss the choice of to obtain high-quality reconstruction results. Then, is multiplied by the intensity of the rectangular aperture to form the complex amplitude:

$$g_0 = \sqrt{I_0}\exp\left(j\varphi_0\right) \tag{12}$$

Here, I_0 is a binary function where the region with 1 in the center, it is the signal area. The non-signal region is the region with 0 around the signal area. The resolution of the signal region is $m \times n$, the resolution of the whole image including the non-signal region is $M \times N$, which is also shown in Fig. 5.

Therefore, by Step 1, the initial value for iteration is obtained.

Step 2: Obtain the optimized hybrid phase φ' through iteration.

The g_0 is used as the initial value for the iterative process, obtain the G_k through IDF and k is the number of iterations. Considering that energy is conserved, the energy of the hologram plane should be the same as that of the image plane. Unlike the GS algorithm, $\left|G_k\right|$ is not simply replaced by 1, but is constrained in the following way:

$$\left|G'_k\right| = \sqrt{\frac{\sum_{x=1}^{M}\sum_{y=1}^{N}\left|I_0\right|^2}{MN}} \tag{13}$$

$\left|G'_k\right|$ is the constrained amplitude of the hologram, where M and N represent the resolution of the signal area in the x and y directions. This processing can concentrate the energy in the signal area, improve diffraction efficiency, and thereby enhance the quality of reconstruction.

The G'_k undergoes FD and arrives at the image plane, resulting in g'_k. On the image plane, the amplitude of the signal region is constrained, while the non-signal region is unconstrained. Thus, $\left|g_{k+1}\right|$ is obtained as the initial value for the next iteration:

$$\left|g_{k+1}\right| = \begin{cases} \left|\sqrt{I_0}\right| \cdot \left(\dfrac{\left|\sqrt{I_0}\right|}{\left|g'_k\right| + c}\right)^{\alpha}, & signal\ region \\ \left|g'_k\right|, & non-signal\ region \end{cases} \tag{14}$$

By only constraining in the signal area, the computational burden can be reduced. After k iterations, an optimized hybrid phase hologram φ' can be obtained.

Step 3: Obtain POHs through one calculation.

The optimized hybrid phase φ' is multiplied by the target image amplitude $\left|A_{targ}\right|$ to form complex amplitude. After undergoing IFD, the phase ψ of G' is extracted, which is the POH. Based on this POH, reconstruction image amplitude $\left|A_{re}\right|$ can be obtained with just one FD.

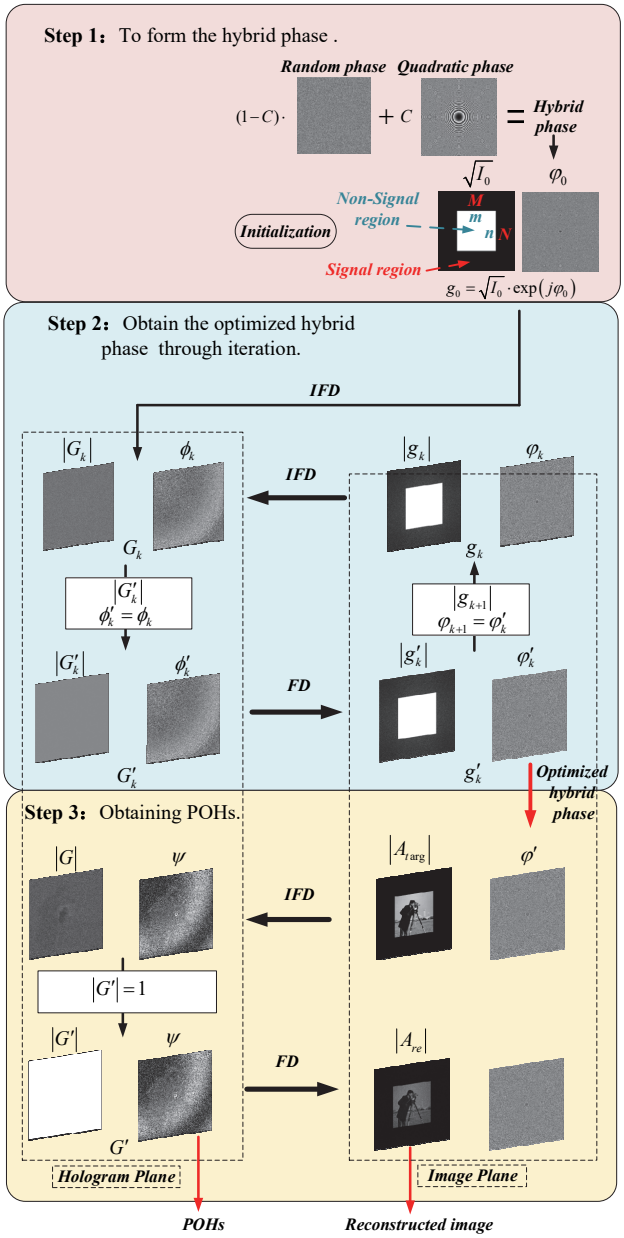

Figure 5 OHPOH algorithm flowchart

4 EXPERIMENT RESULTS AND ANALYSIS

The reconstructed images generated by OHPOHs, ORAP, and HPOHS will be compared.The target image used was "cameraman", as shown in Fig. 3a. In order to evaluate the quality of the reconstruction, we used Root Mean Square Error (*RMSE*) as the evaluation parameter, which is defined as follows:

$$RMSE = \sqrt{\frac{1}{MN}\sum_{p=1}^{M}\sum_{q=1}^{N}\left[\left|A_{re}(p,q)\right| - \left|A_{targ}(p,q)\right|\right]^2} \tag{15}$$

$\left|A_{re}(p,q)\right|$ and $\left|A_{targ}(p,q)\right|$ are the intensity distributions of the reconstruction and the target. The lower the *RMSE* value, the better the reconstruction quality.

Here, our computer processor is CORE i7-8550U, and the computing software is MATLAB R2018b.The resolution of the hologram is set to 1200 × 1200, with a pixel size of 9.2 μm. The d is 40 mm, and the λ is set to

532 nm. The resolution of the image plane is also 1200 × 1200, with a central signal region of 600 × 600 sampling points, and what size the rectangular aperture should be set will be discussed later. According to Eq. (10), the parameter r of the quadratic phase is determined. The change of the weighting coefficient C will cause the change of the hybrid phase φ_0. We multiplied the target image with optimization hybrid phase masks obtained with different weight coefficient C to obtain a series of reconstructed images. The closer the C is to 1, the closer the φ_0 is to random phase; the closer the C is to 0, the closer the φ_0 is to quadratic phase. φ_0 is optimized to φ' and multiplied with the target image mask. The threshold of C is from 0 to 1 with a step size of 0.2, and the iteration number k is 50.

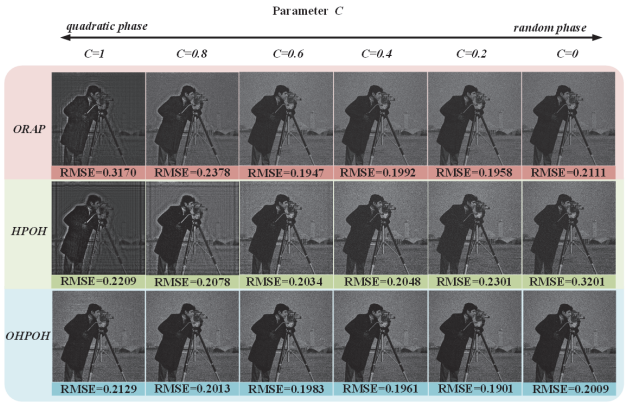

Figure 6 Comparison of reconstructed images generated by ORAP algorithm, HPOH algorithm, and OHPOH algorithm with different weight coefficients C

Fig. 6 displays the "cameraman" iamge used as the target in the experiment. The OHPOHs and the ORAP employ the phase mask calculation methods described in Eq. (11), while the HOPHs utilizes the hybrid phase defined in Ref (24).

Fig. 6 indicates the influence of initial quadratic phase and random phase on reconstruction. It can be observed that as the C approaches 1, both the ORAP and the HPOHs show obvious ringing artifacts in the reconstructed images, which are caused by quadratic phase. However, the ringing artifacts produced by the OHPOHs are not very noticeable. As the C approaches 0, the influence of ringing artifacts decreases while speckle noise becomes more prominent. When C is set to 0.2, the OHPOHs achieves the best reconstruction performance with an *RMSE* value of 0.1901.

To provide a clearer comparison of these three algorithms, we extracted the best reconstruction results for each algorithm from Fig. 6, as shown in Fig. 7. It can be seen that the OHPOHs has the best reconstruction performance among the three algorithms. Therefore, the significant advantage of OHPOHs lies in its ability to effctively reduce speckle noise and ringing artifacts while optimizing details. The reason for this is that most images have both high-frequency and low-frequency components, and the optical wave cannot be uniformly distributed on the hologram plane, so only high-frequency components are usually reconstructed, while low-frequency components are lost. Adding random phase can make the object wave uniformly recorded on the hologram, and low-frequency signals can be preserved, but this will also bring speckle noise; adding quadratic phase can make the spectrum of the object wave smoother. By iteratively optimizing the hybrid phase, the phase distribution can be smoothed, and the diffraction characteristics of the random phase can be reduced, thereby improving the reconstructed quality.

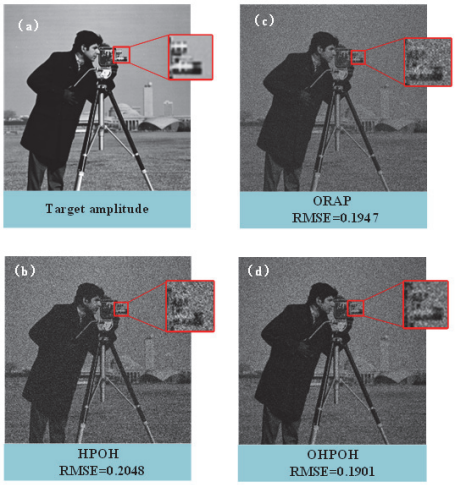

Figure 7 Comparison of details in the reconstructed images obtained by the three algorithms: (a) original image; (b) ORAP algorithm; (c) HPOH algorithm; (d) OHPOH algorithm

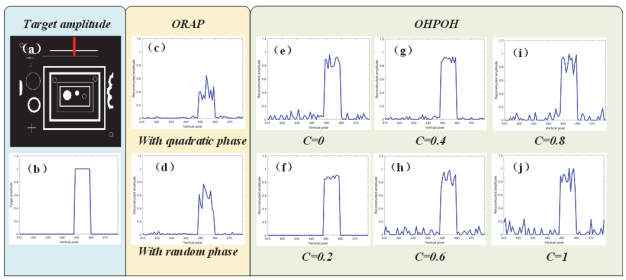

Figure 8 (a) The original image with a red line; the amplitude of the red segment with (b) the original image; (c-d) the reconstructed images generated by the ORAP algorithm using the quadratic and random phase mask; (e-j) the reconstructed images generated by the OHPOH algorithm at different weight coefficients C

Based on the above expeiments, it can be observed that OHPOHs achieves better reconstructed results compared to ORAP and HPOHs. The selection of coefficient C is crucial as it determines the proportion of the two hybrid phases. In order to better study the influence of C on the reconstruction effect, we use binary image "blobs" as the target image, and study the amplitude distribution at the red line segment (1 × 70 pixel), as shown in Fig. 8a and Fig. 8b shows the amplitude at the red line segment of the target image, and Fig. 8c and Fig. 8d depic the amplitude at the marked red line for the reconstructed images obtainded by ORAP algorithm using a random and quadratic phase mask, respectively. It can be seen that its amplitude differs significantly from the target amplitude, with an amplitude size that is 40% - 60% smaller, indicating low energy propagation efficiency. Fig. 8e and Fig. 8j show the amplitude distribution at the marked red line for the reconstructed images generated by the OHPOHs using different coefficients C. It is easy to see that their amplitudes are similar to Fig. 8b, indicating high energy propagation efficiency. It can also shows that when the coefficient C approaches 1 or 0, the waveform becomes oscillatory and uncontrollable, while when it is 0.2 and 0.4, the waveform is relatively smooth and tends towards the target amplitude distribution. The reason for this outcomes is that most images inevitbaly contains both

high-frequency componets and low-frequency componets. The distribution of light waves ong the hologram plane is not uniform, resulting in the easier reconstruction of high-frequency compnets while low-frequency compenents are more prone to be lost. Therefore, this indicates the importance of coefficient C, as it influences the effectiveness of suppressing ringing artifacts and speckle noise.

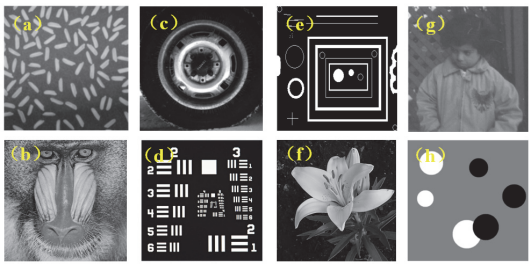

Figure 9 (a-h) Test images

The study of the value of coefficient C above is relatively rough, and using only one test image cannot objectively and accurately study the effect of C on the reconstruction. Therefore, eight test images were used, as shown in Fig. 9, to study the effect of the value of C using the *RMSE* value between the target amplitude and the reconstructed amplitude as an indicator.

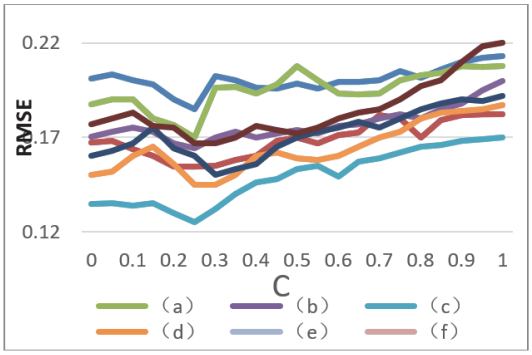

Figure 10 *RMSE* values between the eight test images and their reconstructed images with different settings of the weight coefficient C

In the experiment, the range of the coefficient C is from 0 to 1, with values taken at intervals of 0.05, except for the replacement of the target image, the settings of other parameters are the same as in the previous text. The *RMSE* curves for each target image are shown in Fig. 10, where the horizontal axis represents the values of the C, and the vertical axis represents the *RMSE* value. Although the eight curves have fluctuations, their trends are basically consistent. When the coefficient C is set to 0, the reconstruction quality is poorer, primarily due to the influence of speckle noise. With the increase of C, the reconstruction quality becomes better, reaching the lowest point of the curve between 0.2 and 0.3, that is, the reconstruction quality is optimal. The reason is that the increase of the quadratic phase ratio makes the phase distribution smoother, thereby suppressing the speckle noise. As the value of C increases, the reconstruction quality deteriorates due to the influence of ringing artifacts caused by the quadratic phase. Therefore, the optimal choice for C is between 0.2 and 0.3, which can combine the advantages of random phase masks and quadratic phase masks and achieve better reconstruction for most target images. Therefore, we set the weight coefficient C to the middle value of 0.25.

To further evaluate the effectiveness of the algorithm, we will also employ the diffraction efficiency η as an indicator. Its calculation formula is:

$$\eta = \frac{E_{re\_signal}}{E_{holo\_signal} + E_{holo\_noise}} \tag{16}$$

That is, the η is the energy ratio of the signal area of the reconstructed image E_{re_signal} to the total energy of the incident light $E_{holo\_signal} + E_{holo\_noise}$ on the hologram. We need to compare the η and *RMSE* values of the reconstructed images generated by the three algorithms. The coefficient C for OHPOHs is set to the optimal value of 0.25, which has been validated through the experiments conducted earlier, and the remaining experimental parameters are set consistently with the setting for previous experiments. The HPOHs uses C as 0.35, which is the optimal value analyzed in Ref [24]. The ORAP uses quadratic phase and random phase as initial phases, and the reconstruction and POHs are shown in Fig. 11.

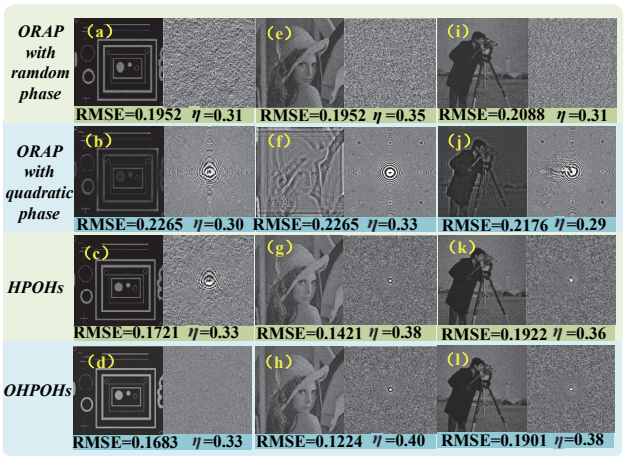

Figure 11 Reconstructed amplitude, POHs, diffraction efficiency η, and *RMSE* values generated using (a), (e), (i) ORAP with random phase masks; (b), (f), (j) ORAP with quadratic phase masks; (c), (g), (k) HPOHs; (d), (h), (l) OHPOHs.

Fig. 11. shows the reconstructed amplitudes and obtained POHs using these three algorithms. It can be observed that for the ORAP, if a random phase mask is used, the reconstructed amplitude will have more speckle noise; if a quadratic phase mask is used, the reconstructed amplitude will have severe ringing artifacts, which lead to a decrease in diffraction efficiency and an increase in *RMSE* value. The HPOHs has a significant improvement compared to the ORAP algorithm, but the reconstructed amplitude obtained by the OHPOHs has better reconstruction quality compared to the HPOHs, with the highest diffraction efficiency and a smoother distribution of POHs. OHPOHs achieved the best reconstruction results compared to HPOHs and ORAP. It also exhibited the highest diffraction efficiency with a smoother distribution of POHs.

Another advantage of the OHOPHs algorithm is its low time consumption, which means what only we need is to obtain the relevant parameters of an optical system, such as the resolution and pixel size of SLMs, and propagation

distance, in order to iteratively calculate and generate optimized phases. For this optical system, the optimized phase only needs to be generated once, and can be combined with any target image to form a complex amplitude. By performing a single IFD calculation, the OHPOHs algorithm can obtain POHs, significantly reducing time consumption for generating POHs. Tab. 1 compares the computation time of ORAP, HPOHs and OHPOHs. In the numerical experiments, the k was set to 50, and the resolution of the entire image was set to 1200 × 1200 and 600 × 600, other parameters unchanged. The computer processor used was CORE i7-8550U, and the calculation software used was MATLAB R2018b. The "+" in the table represents the time spent on optimizing the phase plus the time spent on generating POHs in one calculation. For example, "5.83 + 0.48" means that the time cost of calculating the optimized phase is 5.53 s, and the time cost of calculating the POHs in one step according to the obtained optimized phase is 0.48 s.

Table 1 Comparison of time cost of the three algorithms under different resolutions

Resolution pixel s	ORAP	HPOHs	OHPOHs
600 × 600	5.76 + 0.56	1.23	5.83 + 0.48
1200 × 1200	17.63 + 0.77	5.43	17.88 + 0.62

As can be seen from Tab. 1, the total time consumption of ORAP and OHPOHs is similar. Although ORAP has a shorter time for generating optimized phase, OHOPHs can generate POHs faster. HPOHs have the smallest total time consumption because the algorithm does not involve an iterative process for optimizing the initial phase. It only requires a single convolution calculation to generate POHs. However, the OHPOHs algorithm can compute the optimized phase before generating images, allowing for a faster generation of POHs, which requires lower time overhead compared to time overhead for generating POHs in HPOHs.

Therefore, the advantage of the OHPOHs is that once the optimized phase is pre-generated, POHs can be quickly generated, providing new ideas for real-time display and 3D display. However, the OHPOHs still has some limitations. This algorithm is suitable for near-field diffraction, and exploring the method of increasing diffraction distance is one of the directions of further exploration.In addition, FD still involves *FFT* calculations, which will greatly affect the calculation speed. Fourier lens can be used instead of *FFT* calculation process, but this will cause the complexity of the optical path. How to balance the complexity of the optical path and the computational complexity is worth considering.

5 CONCLUSION

In this paper, we begin by analyzing the reasons for speckle noise and ringing artifacts introduced by random phase and quadratic masks respectively for generating in ORAP algorithm. To address these issues, we propose a non-iterative algorithm, which can genrerate POHs through three steps, based on optimized hybrid phase specifically designed for Fresnel Lensless Holographic projection systems.

One notable advantage of this algorithm is the relatively smooth phase distribution observed in the generated POHs, which effectively suppresses speckle noise and ringing artifacts, resulting in high diffraction efficiency and high-quality reconstructed images. Furthermore, the algorithm offers another advantage faster generation of POH, which means the algorithm can compute the optimized phase before generating images, resulting in fast generation of POHs for different target images. Numerical experiments have also been conducted to validate the overwhelming advantages of this algorithm.

In addition, this algorithm can be applied to more fields, such as fast holographic 3D reconstruction and real-time holographic projection. In the follow-up research, we will consider how to further improve the computational efficiency and expand the diffraction distance.

Acknowledgements

This work is supported by the National Science Foundation (61302179), the Universities Natural Science Research Foundation of Anhui province (KJ2019A0619, KJ2020A0091, 2022AH052119), the Science Research Foundation of Hefei Normal University (2022KJZD02), the Provincial Scientific Research Platform Special Program of Hefei Normal University (2020PT11), Enterprise Commissioned Development Project of Anhui Province (HXXM2022040, 2022HXXM155), Natural Science Foundation of Anhui University (2022AH052135) and Undergraduate Teaching Quality Project in Anhui Province (2020SJJXSFK1985). The financial support provided by them is greatly appreciated.

6 REFERENCES

[1] Gabor, D. (1948). A new microscopic principle. *Nature*, *161*(4098), 777-778. https://doi.org/10.1038/161777a0

[2] Wang, H., Shan, Y., & Zheng, D. (2022). The real-time dynamic holographic display of LN:Bi, Mg crystals and defect-related electron mobility. *Opto-Electronic Advances*, *5*(12), 4-12. https://doi.org/10.29026/oea.2022.210135

[3] Chao, Y., Xiangyu, M., Jiang, L., Cai, H., Mao, H., Wang, R., & Pu, S. (2023). Holographic Near-Eye Display System with Expanded Eyebox Based on Waveguide. *Acta Optica Sinica*, 1-23.

[4] Zhang, S., Huang, L., & Geng, G. (2022). Full-Stokes polarization transformations and time sequence metasurface holographic display. *Photonics Research*, *10*(4), 1031-1038. https://doi.org/10.1364/PRJ.450354

[5] Wang, D., Liu, C., Shen, C., Xing, Y., & Wang, Q. H. (2020). Holographic capture and projection system of real object based on tunable zoom lens. *PhotoniX*, *1*(1), 110-117. https://doi.org/10.1186/s43074-020-0004-3

[6] Kang, H., Yamaguchi, T., & Yoshikawa, H. (2008). Accurate phase-added stereogram to improve the coherent stereogram. *Applied Optics*, *47*(19), D44-D54. https://doi.org/10.1364/AO.47.000D44

[7] Lin, S. F., Cao, H. K., & Eun-Soo, K. (2019). Single SLM full-color holographic three-dimensional video display based on image and frequency-shift multiplexing. *Optics Express*, *27*(11), 15926-15942. https:/doi.org/10.1364/OE.27.015926

[8] Slinger, C., Cameron, C., & Stanley, M. (2005). Computer-generated holography as a generic display technology. *Computer*, *38*(8), 46-53. https:/doi.org/10.1109/MC.2005.260

[9] Zhang, H., Cao, L., & Jin, G. (2019). Three-dimensional computer generated hologram with Fourier domain

segmentation. *Optics Express*, *27*(8), 11689-11697. https:/doi.org/10.1364/OE.27.011689

[10] Takekawa, Y., Takashima, Y., & Takaki, Y. (2020). Holographic display having a wide viewing zone using a MEMS SLM without pixel pitch reduction. *Optics Express*, *28*(5), 7392-7407. https:/doi.org/10.1364/OE.385645

[11] He, Z., Sui, X., Jin, G., Chu, D., & Cao, L. (2021). Optimal quantization for amplitude and phase in computer-generated holography. *Optics Express*, *29*(1), 119. https:/doi.org/10.1364/OE.414160

[12] Gerchberg, R. W. (1972). A practical algorithm for the determination of phase from images and diffraction plane picture. *Optics*, 35.

[13] Fienup, J. R. (1980). Iterative method applied to image reconstruction and to Computer-Generated Holograms. *Optical Engineering*, *19*(3), 193297. https:/doi.org/10.1117/12.7972513

[14] Kuzmenko, A., Yezhov, P. V., & Kim, J. T. (2011). Weighting Iterative Fourier Transform Algorithm for Kinoform Implemented with Phase-Only SLM. *In Tech*. https://doi.org/10.1364/DH.2011.DTuC37

[15] Wu, Y., Wang, J., Chen, C., Liu, C. J., Jin, F. M., & Chen, N. (2021). Adaptive weighted gerchberg-saxton algorithm for generation of phase-only hologram with artifacts suppression. *Optical Society of America*. https:/doi.org/10.1364/OE.413723

[16] Tao, S. & Yu, W. X. (2015). Beam shaping of complex amplitude with separate constraints on the output beam. *Optics Express*, *23*(2), 1052-1062. https:/doi.org/10.1364/OE.23.001052

[17] Takaki, Y., Yokouchi, M., & Okada, N. (2010). Improvement of grayscale representation of the horizontally scanning holographic display. *Optics Express*, 18(24), 24926-24936. https:/doi.org/10.1364/OE.18.024926

[18] Fan, M., Yang, J., Du, C. T., Fang, J., Wang, H. B., & Li, C. L. (2022). A hybrid iterative algorithm of amplitude weighting and phase gradient descent for generating phase-only fourier hologram. *Traitement du Signal*, *39*(5), 1789-1796. https://doi.org/10.18280/ts.390538

[19] Lohmann, A. W. & Paris, D. P. (1967). Binary Fraunhofer holograms, generated by computer. *Applied Optics*, *6*(10), 1739-1748. https://doi.org/10.1364/AO.6.001739

[20] Chen, L., Tian, S., Zhang, H., Cao, L., & Jin, G. (2021). Phase hologram optimization with bandwidth constraint strategy for speckle-free optical reconstruction. *Optics Express*, *29*(8), 11645-11663. https://doi.org/10.1364/OE.422115

[21] Velez, Z. A., Ramirez, B. J. F., & Torroba, R. (2018). Optimized random phase only holograms. *Optics Letters*, *43*(4), 731-734. https://doi.org/10.1364/OL.43.000731

[22] Velez-Zea, A. & Torroba, R. (2019). Optimized random phase tiles for non-iterative hologram generation. *Applied Optics*, *58*(32), 9013-9019. https://doi.org/10.1364/AO.58.009013

[23] Chen, L. Z., Zhang, H., Gao, L. C., & Jin, G. F. (2020). Non-iterative phase hologram generation with optimized phase modulation. *Optics Express*, *28*(8), 11380-11392. https://doi.org/10.1364/OE.391518

[24] Shen, C., Qi, Y. F., Lv, S. Q., Wang, B., & Wei, S. (2022). Generation of non-iterative phase-only hologram based on a hybrid phase mask. *Applied Optics*, *61*(6), 1507-1515. https://doi.org/10.1364/AO.449555

[25] Zhang, C., Hu, Y., Li, J., Lao, Z., & Dong, W. (2014). An improved multi-exposure approach for high quality holographic femtosecond laser patterning. *Applied Physics Letters*, *105*(22), 221104. https://doi.org/10.1063/1.4902925

[26] Alsaka, C. (2018). A comparison of iterative Fourier transform algorithms for image quality estimation. *Optical Review*, *25*(5), 625-637. https://doi.org/10.1007/s10043-018-0456-x

[27] Mehrabkhani, S. & Kuester, M. (2017). Optimization of phase retrieval in the fresnel domain by the modified gerchberg - saxton algorithm.

[28] Yan, Z., Gao, L., Zhang, H., Tan, W., Wu, S., Wang, Z., Yang, Q., & Jin, Q. (2016). Time-division multiplexing holographic display using angular-spectrum layer-oriented method (Invited Paper). *Chinese Optics Letters*, *14*(1), 20-24. https://doi.org/10.3788/COL201614.010005

[29] Mori, Y., Fukuoka, T., & Nomura, T. (2014). Speckle reduction in holographic projection by random pixel separation with time multiplexing. *Applied Optics*, *53*(35), 8182-8188. https://doi.org/10.1364/AO.53.008182

[30] Chen, C., He, M. Y., Wang, J., Chang, K. M., & Wang, Q. H. (2019). Generation of phase-only holograms based on aliasing reuse and application in holographic see-through display system. *IEEE Photonics Journal*, *11*(3), 1-11. https://doi.org/10.1109/jphot.2019.2911981

[31] Velez-Zea, A., Barrera, R., John, F., & Torroba, R. (2022). Improved phase multiplexing using iterative and non-iterative hologram generation. *Optics and Lasers in Engineering*, 151. https://doi.org/10.1016/j.optlaseng.2021.106921

[32] Tsang, P., Chow, Y. T., & Poon, T. C. (2016). Generation of complementary sampled phase-only holograms. *Optics Express*, *24*(20), 23390-23395. https://doi.org/10.1364/OE.24.023390

[33] Yoshikawa, N. & Yatagai, T. (1994). Phase optimization of a kinoform by simulated annealing. *Applied Optics*, *33*(5), 863-868. https://doi.org/10.1364/AO.33.000863

[34] Leportier, T., Park, M. C., Kim, Y. S., & Kim, T. (2015). Converting optical scanning holograms of real objects to binary Fourier holograms using an iterative direct binary search algorithm. *Optics Express*, *23*(3), 3403-3411. https://doi.org/10.1364/OE.23.003403

[35] B., H. W. A., B., W. Y. A., B., Q. S. A., C., J. L. A., & A., G. S. (2017). A hybrid gerchberg–saxton-like algorithm for doe and cgh calculation. *Optics and Lasers in Engineering*, 89, 109-115. https://doi.org/10.1016/j.optlaseng.2016.04.005

[35] Jun, W., Xiang, L. L., Yang, W., Fengming, J., & Ni, C. (2022). Holographic display with optical computational Fresnel convolution to broaden distance, *Optics Express*, *30*(3) 4288-4301. https://doi.org/10.1364/OE.450778

[36] Yan, Z., Gao, L., Zhang, H., Tan, W., Wu, S., Wang, Z., Yang, Q., & Jin, Q. (2016). Time-division multiplexing holographic display using angular-spectrum layer-oriented method (Invited Paper). *Chinese Optics Letters*, *14*(1), 20-24. https://doi.org/10.3788/COL201614.010005

[37] Tian, S., Chen, L., & Zhang, H. (2022). Optimized Fresnel phase hologram for ringing artifacts removal in lensless holographic projection. *Applied Optics*, *61*(5), B17-B24. https://doi.org/10.1364/AO.441095

[38] Shimobaba, T., Makowski, M., Takahashi, T., Yamamoto, Y., & Ito, T. (2020). Reducing computational complexity and memory usage of iterative hologram optimization using scaled diffraction. *Applied Sciences*, *10*(3). https://doi.org/10.3390/app10031132

[39] Zea, A. V. (2021). Iterative multiplane hologram generation with mixed constraint. *Applied Optics*, *60*(2), 224-231. https://doi.org/10.1364/AO.408402

[40] Voelz, D. G. & Roggemann, M. C. (2009). Digital simulation of scalar optical diffraction: Revisiting chirp function sampling criteria and consequences. *Applied optics*. https://doi.org/10.1364/AO.48.006132

Contact information:

Min FAN, Master, Lecture
AnHui Province Key Laboratory of simulation and design for Electronic information system,
Hefei Normal University,
Hefei, China 230061
School of Electronic and Electrical Engineering,
Hefei Normal University,
Hefei, China 230061
E-mail: fanmin@hfnu.edu.cn

Jiaxuan WANG, Junior students
School of Electronic and Electrical Engineering,
Hefei Normal University,
Hefei, China 230061
E-mail: wangjiaxuan@hfnu.edu.cn

Chengtao DU, Master, Associate Professor
(Corresponding author)
Department of Electrical and Photo Engineering,
West Anhui University,
Lu'an, China 237012
E-mail: ctdu@wxc.edu.cn

Jin YANG, PhD, Associate Professor
(Corresponding author)
School of Electronic and Electrical Engineering,
Hefei Normal University,
Hefei, China 230061
E-mail: yangjin108@163.com

Haibo WANG, Phd, Associate Professor
School of Electronic and Electrical Engineering,
Hefei Normal University,
Hefei, China 230061
E-mail: john20140105@163.com

Xiaoli XU, Master, Lecture
School of Electronic and Electrical Engineering,
Hefei Normal University,
Hefei, China 230061
E-mail: lilyxu@hfnu.edu.cn